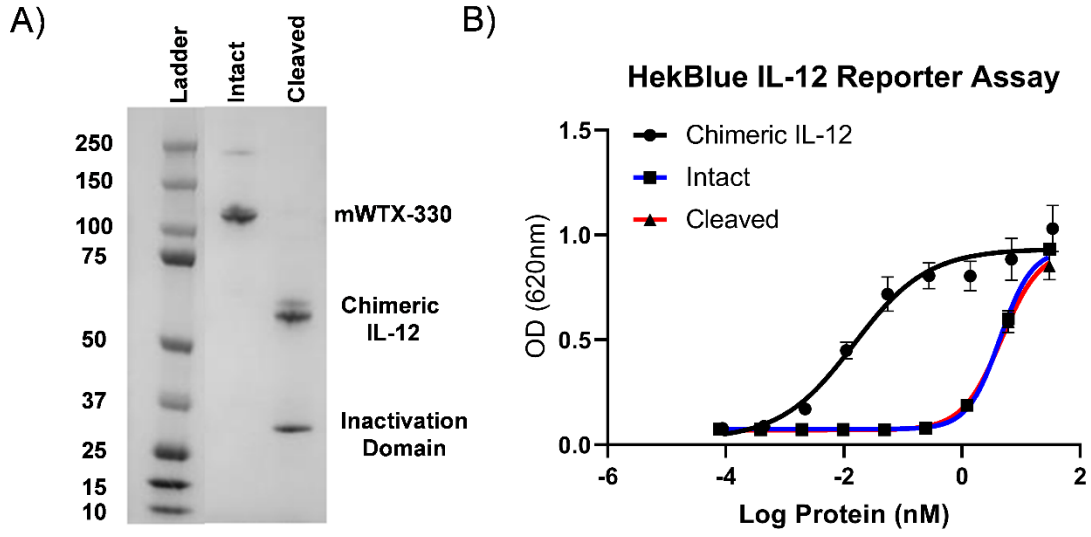
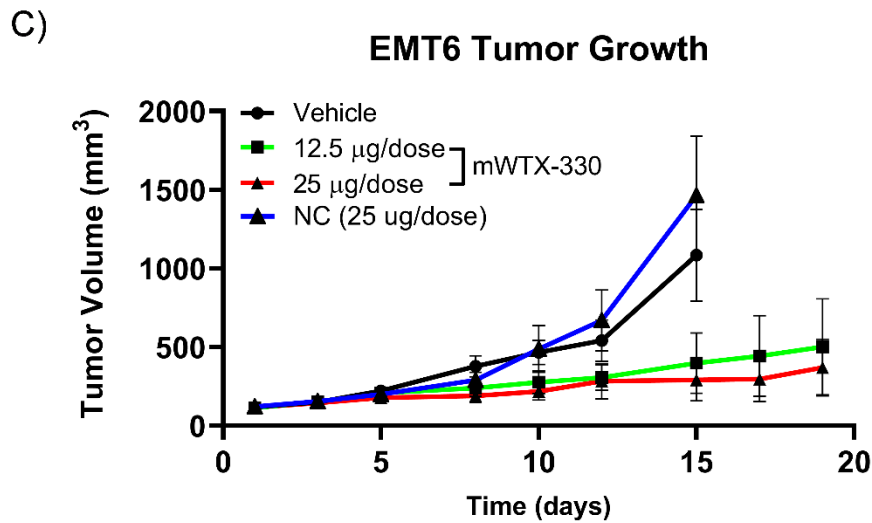


Supplemental Figures

Supplemental Figure 1



\*Half-Life Extension Domain is Too Small for this Gel

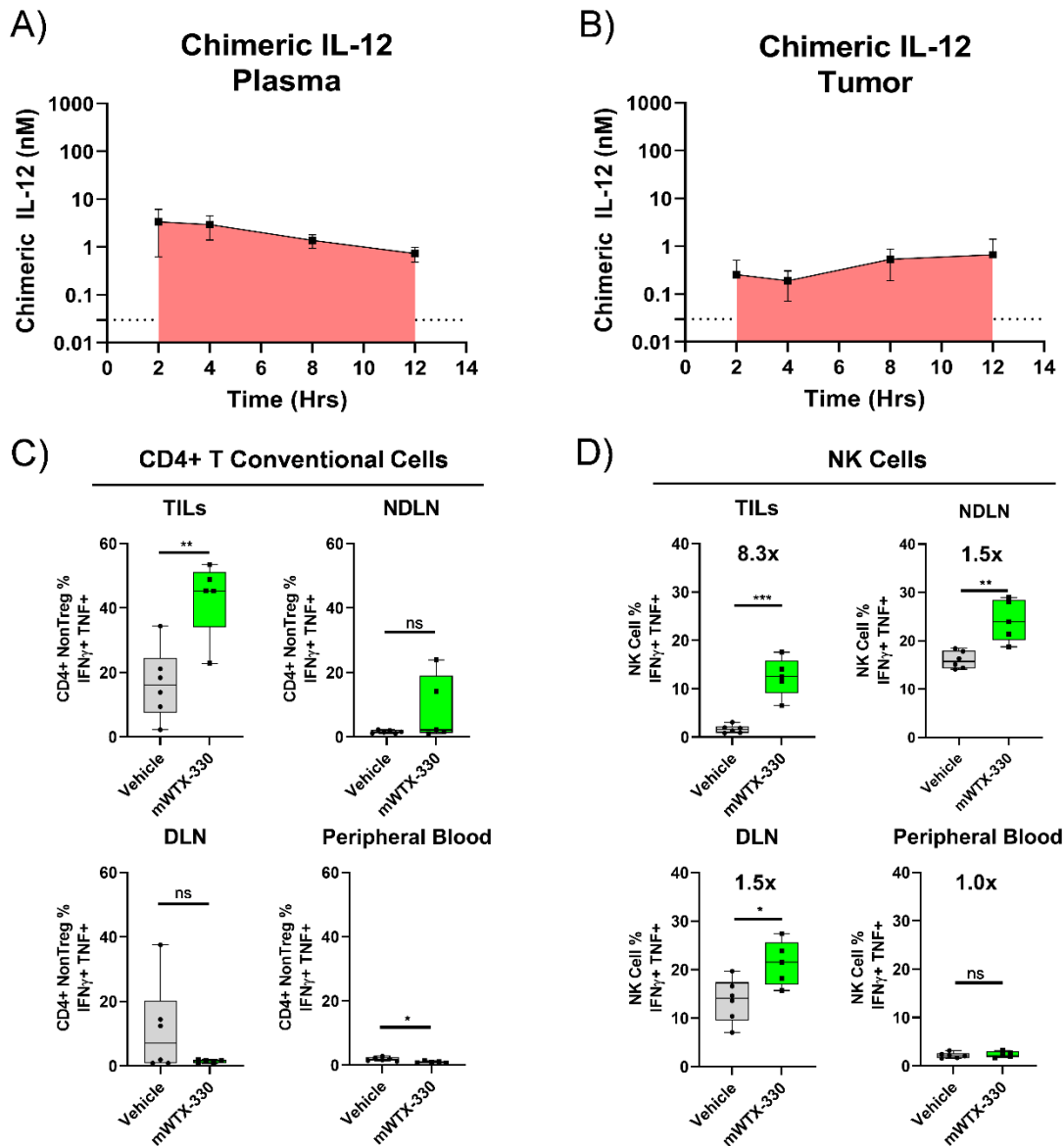


**Supplemental Figure 1: Non-Cleavable Variant of mWTX-330 Remains in the Pro-Drug Format After Exposure to Enzymatic Processing**

**A)** SDS PAGE analysis of mWTX-330 either intact or after *in vitro* activation. **B)** *In vitro* activity of the non-cleavable variant of mWTX-330 (mWTX-330-NC) in the HEK-Blue IL-12

reporter assay comparing intact (blue) and protease-activated (cleaved) mWTX-330-NC (red) to chimeric IL-12 (black). Protease activated mWTX-330-NC was exposed to Cathepsin as reported in the materials and methods for other cleaved INDUKINE molecules. Data are representative of the mean  $\pm$  SD. Tumor growth curves of **C**) EMT-6 tumors. Mice were dosed twice a week for 2 weeks, with the specific doses reported in the figure. Data are representative of the mean  $\pm$  SEM.

## Supplemental Figure 2

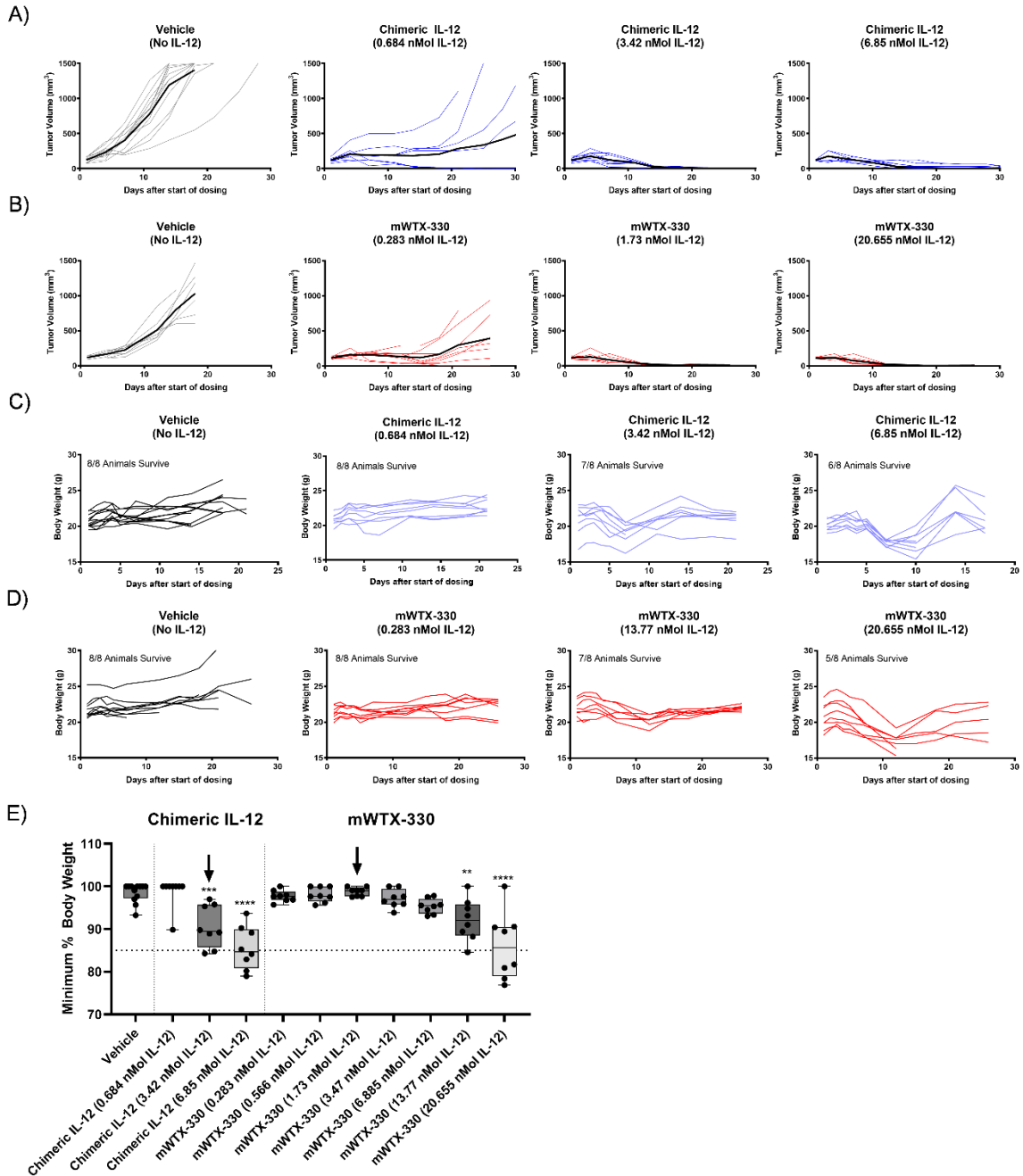


### Supplemental Figure 2: Chimeric IL-12 Exposure and Selective Activation of Tumor Infiltrating Immune Cells

(A-B) MC38 tumor-bearing mice were treated with a single dose of recombinant chimeric IL-12 before (A) plasma and (B) tumor samples were analyzed at various timepoints for the presence of chimeric IL-12 (red). MC38 tumor-bearing mice were treated with two doses of mWTX-330

and **(C)** the frequency of CD4<sup>+</sup> T conventional cells or **(D)** NK cells producing IFN $\gamma$  and TNF in the tumor, peripheral blood, non-tumor draining lymph node, or tumor draining lymph node was measured after PMA/Ionomycin restimulation. Data are presented a box and whiskers plot, with the box representing the 25-75<sup>th</sup> percentile and the middle line representing the group mean, while p values are derived from t tests (\*, p < 0.05; \*\*, p < 0.01; \*\*\*, p < 0.001).

### Supplemental Figure 3

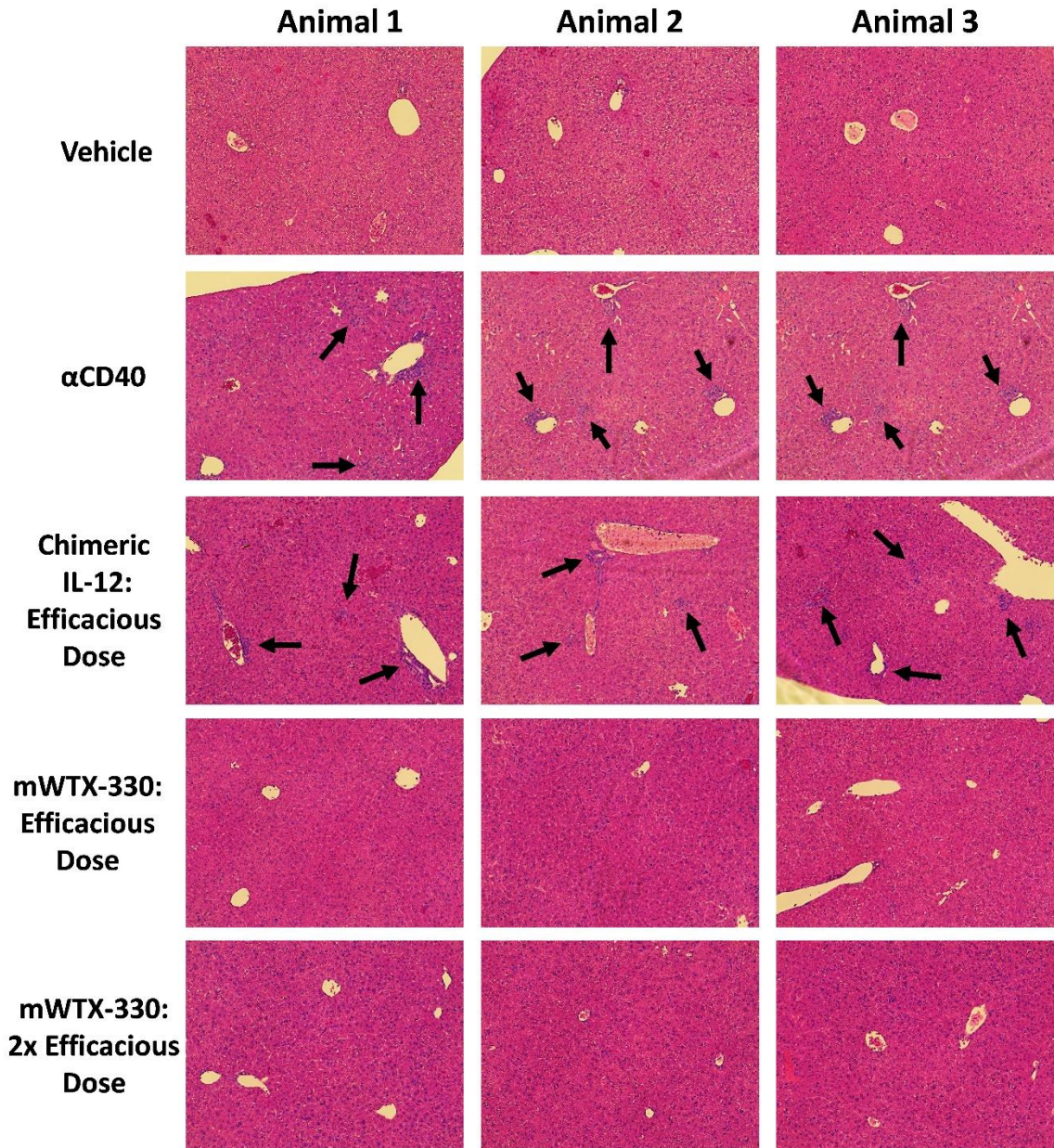


### Supplemental Figure 3: Identification of the MED and MTD in the MC38 Model

MC38 tumor bearing mice were dosed for two weeks, either (A,C) twice a day for 5 days followed by 2 rest days with chimeric IL-12 or (B,D) twice a week with mWTX-330. Doses

were normalized to the moles of IL-12 delivered over the course of treatment. (A-B) Tumor volume and (C-D) body weight was monitored over time, with the bolded line representing the mean tumor volume measurement of the group. E) The minimum percent of the initial body weight over the course of treatment was plotted for individual animals following treatment with either mWTX-330 or chimeric IL-12. A non-tolerable dose was defined as one where animals reached 85% of their initial body weight on average. Arrows indicate the dose required for complete tumor rejection in the MC38 model. Data are presented a box and whiskers plot, with the box representing the 25-75<sup>th</sup> percentile and the middle line representing the group mean, while p values are derived from a 2-way ANOVA with multiple comparisons, comparing each dosing group to the vehicle treated group (\*\*,  $p < 0.01$ ; \*\*\*,  $p < 0.001$ ; \*\*\*\*,  $p < 0.0001$ ).

## Supplemental Figure 4



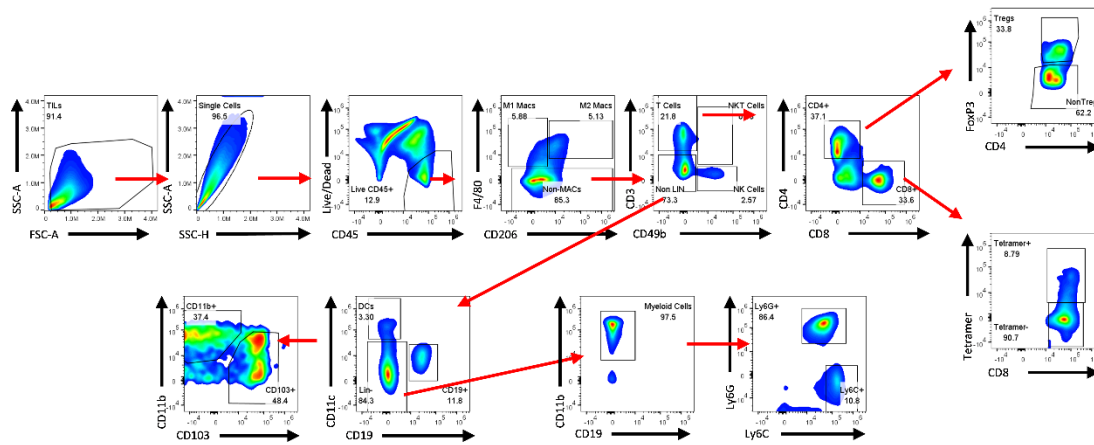
### Supplemental Figure 4: mWTX-330 Does Not Induce Early Liver Dysplasia at the Doses Required for Complete Tumor Rejection

Naïve, 6-8 week old, C57Bl/6 female mice were treated with either vehicle, chimeric IL-12, mWTX-330, or  $\alpha$ CD40 (100  $\mu$ g on Day 0) as a positive control for IL-12 induced liver

infiltration by leukocytes. Mice dosed with chimeric IL-12 received a 10  $\mu\text{g}$  dose twice a day for a total of 5 doses. Mice dosed with mWTX-330 received either 43  $\mu\text{g}$  or 86  $\mu\text{g}$  dosed once on Day 0. Livers were harvested in the afternoon of Day 2. H&E images of murine livers following treatment. Areas of perivenular infiltration by leukocytes or liver dysplasia are marked by arrows.



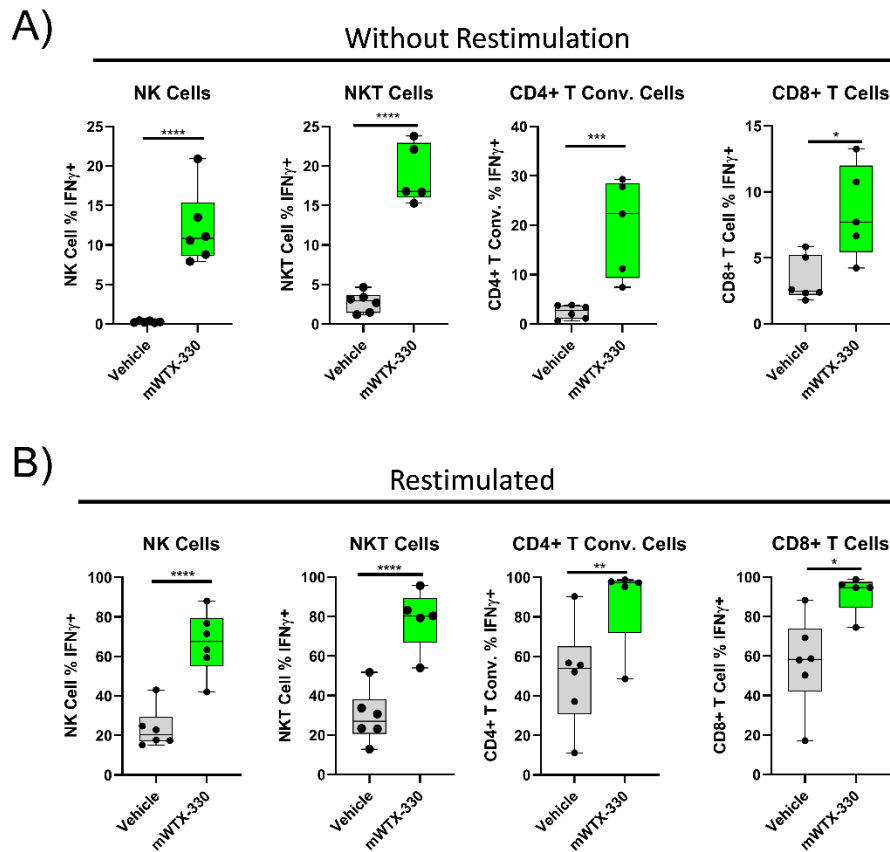
## Supplemental Figure 5



### Supplemental Figure 5: Gating Strategy for the Identification of Various Tumor Infiltrating Immune Cell Populations

Tumors were dissociated into single cell suspensions, and individual immune cell populations were identified using the depicted, representative gating strategy.

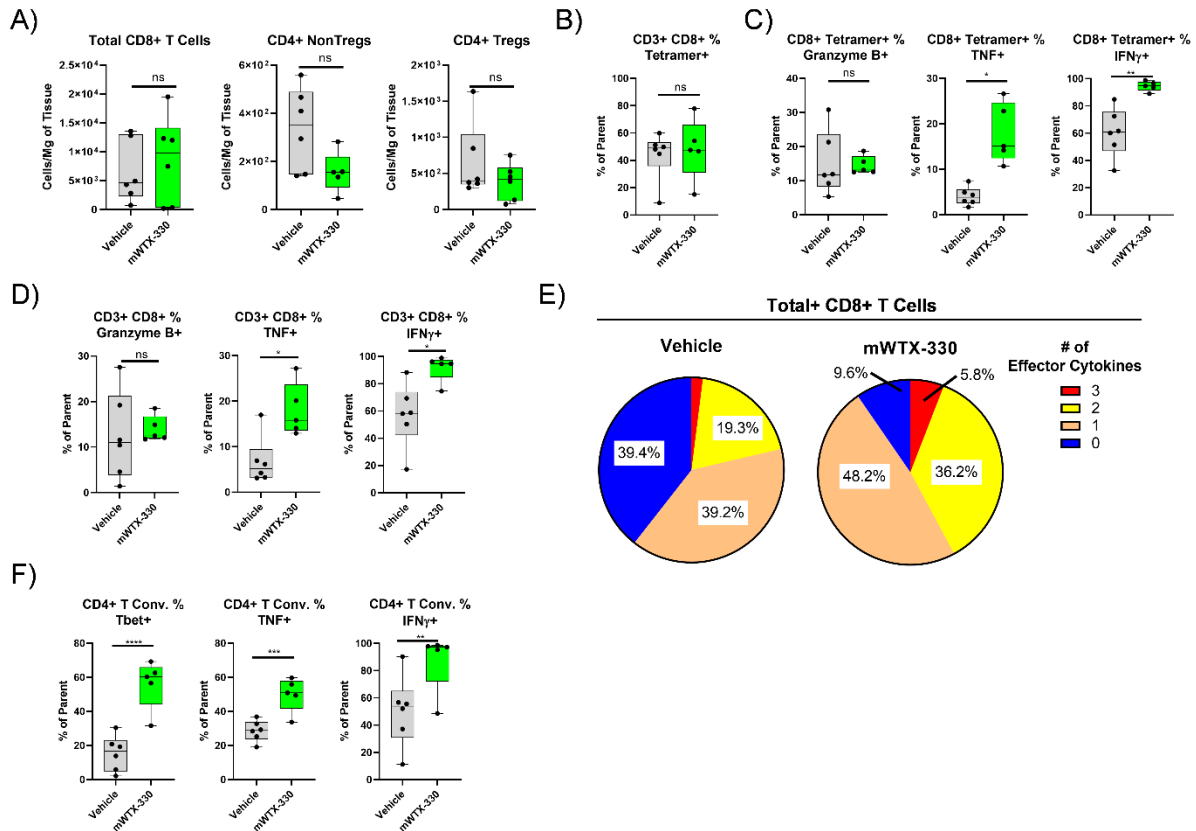
## Supplemental Figure 6



### Supplemental Figure 6: Detection of IFN $\gamma$ Production by Intracellular Cytokine Staining with or without Restimulation

MC38 tumor bearing mice were dosed twice with mWTX-330 or vehicle and tumors were collected 24 hours after the second dose. The production of IFN $\gamma$  by various immune cell populations was assessed by flow cytometry either (A) without restimulation or (B) with PMA/Ionomycin restimulation in the presence of Brefeldin A for 4 hours. Data are presented as a box and whiskers plot, with the box representing the 25-75<sup>th</sup> percentile and the middle line representing the group mean, while p values are derived from t tests (\*,  $p < 0.05$ ; \*\*,  $p < 0.01$ ; \*\*\*,  $p < 0.001$ ; \*\*\*\*,  $p < 0.0001$ ).

## Supplemental Figure 7

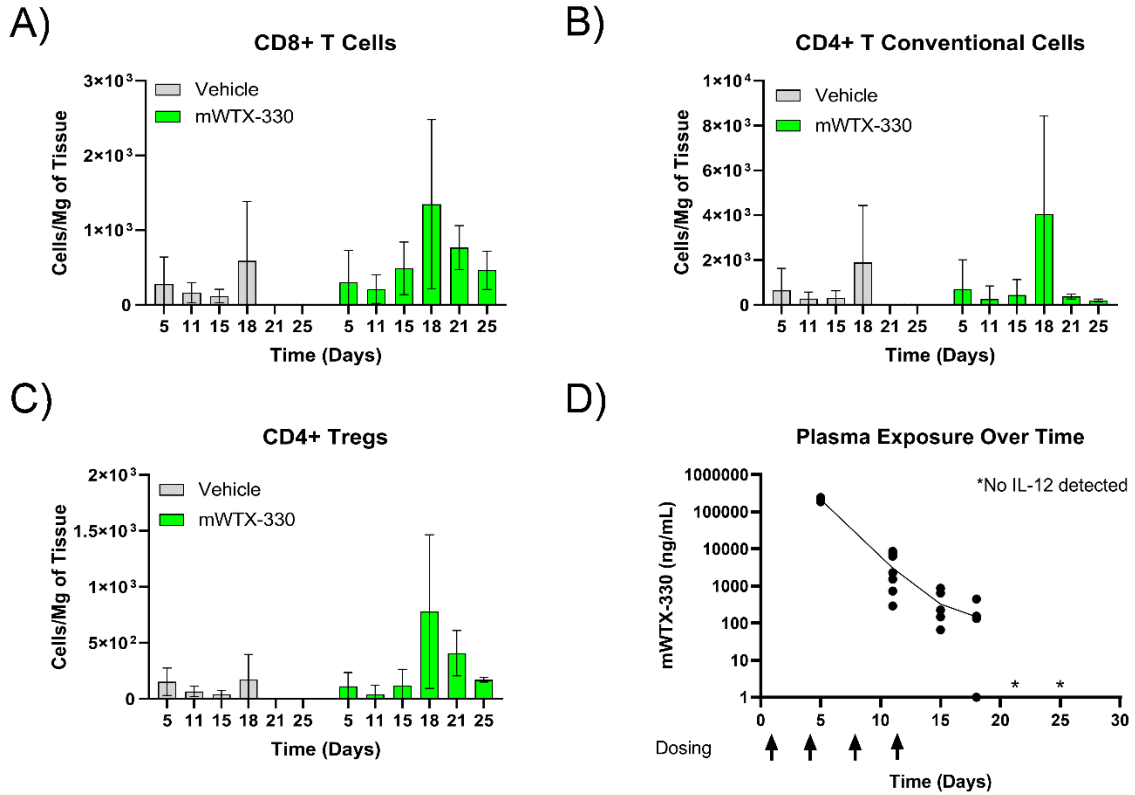


## Supplemental Figure 7: mWTX-330 activates MC38 Tumor Infiltrating TILs

MC38 tumor bearing mice were dosed twice with mWTX-330 or vehicle and tumors were collected 24 hours after the second dose. **(A)** The density of total CD8+ T cells, CD4+ T conventional cells, and CD4+ Tregs within the tumor. **(B)** The frequency of tetramer+ cells among total tumor infiltrating CD8+ T cells. **(C)** The frequency of tumor infiltrating tetramer+ CD8+ T cells producing IFN $\gamma$ , TNF, or Granzyme B. **(D)** The frequency of total CD8+ T cells producing IFN $\gamma$ , TNF, or Granzyme B. **(E)** The frequency of polyfunctional CD8+ T cells was measured by examining co-expression of IFN $\gamma$ , TNF, and Granzyme B after PMA/Ionomycin restimulation. **(F)** The frequency of CD4+ T conventional cells producing IFN $\gamma$ , TNF, or

expressing Tbet. Data are presented a box and whiskers plot, with the box representing the 25-75<sup>th</sup> percentile and the middle line representing the group mean, while p values are derived from t tests (\*,  $p < 0.05$ ; \*\*,  $p < 0.01$ ; \*\*\*,  $p < 0.001$ ; \*\*\*\*,  $p < 0.0001$ ).

## Supplemental Figure 8

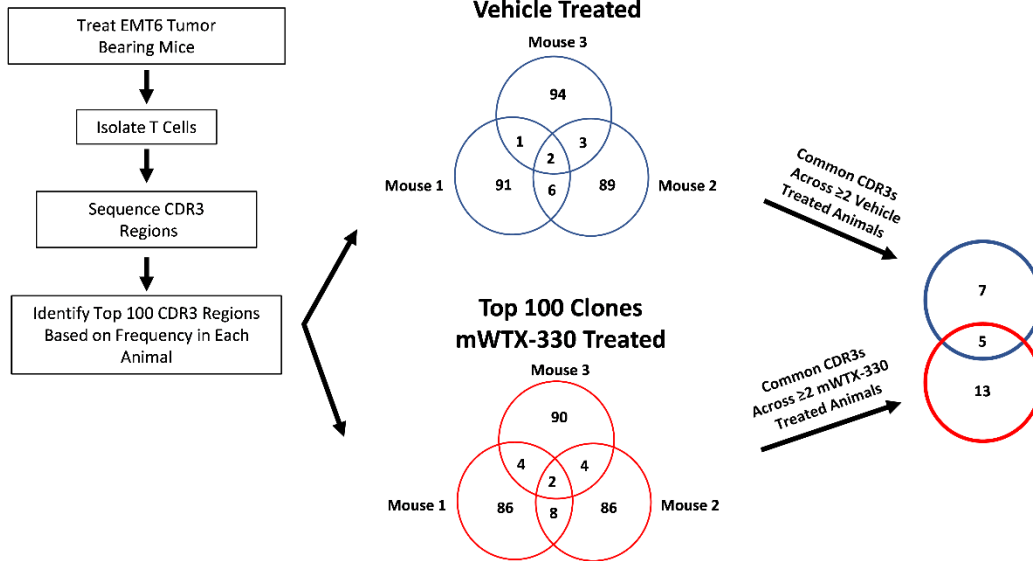


### Supplemental Figure 8: Pharmacodynamic and Pharmacokinetic Analysis of mWTX-330 Exposure in the EMT-6 Model

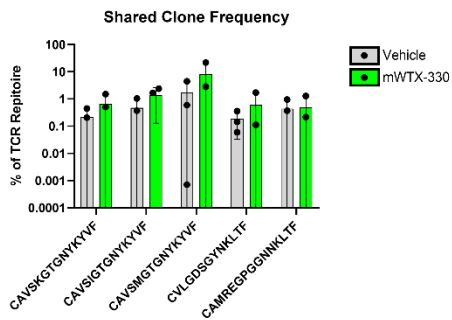
EMT-6 tumor bearing mice were dosed twice a week for two weeks with mWTX-330 or PBS and plasma samples were collected at various time points. (A) The density of total CD8+ T cells, (B) CD4+ T conventional cells, and (C) CD4+ Tregs within the tumor over time. (D) Plasma exposure of total mWTX-330 over time. Doses are indicated by the arrows on the X-axis. Data are presented as the mean  $\pm$  SD.

## Supplemental Figure 9

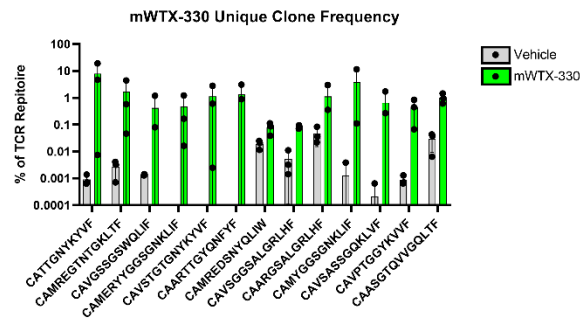
A)



B)



C)

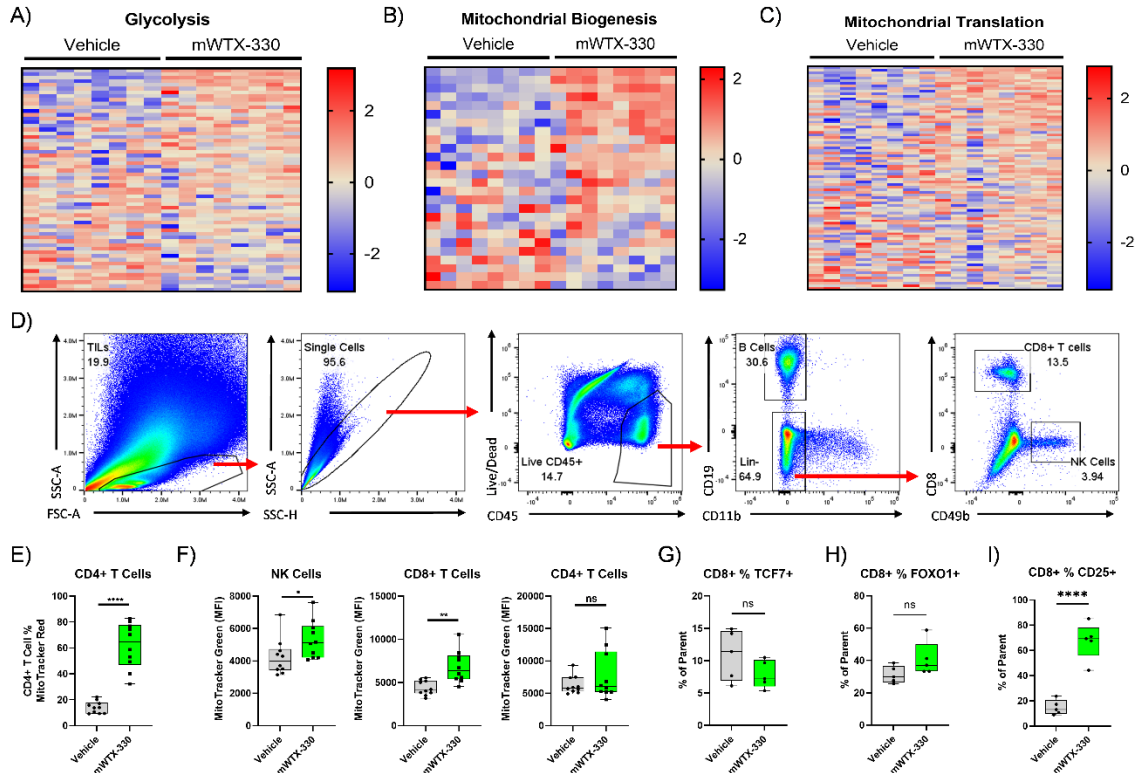


## Supplemental Figure 9: mWTX-330 Preferentially Expands New Clones Rather than Previously Present Clones

EMT-6 tumor bearing mice were dosed twice a week with mWTX-330 or PBS, and tumors were harvested on day 11. Live T cells were enriched using magnetic columns and TCR sequencing was performed. **A)** A diagram of the analysis scheme for comparing common and unique TCR clones between vehicle and mWTX-330 treated animals. **B)** Raw frequencies of individual TCR clones that were identified in the top 100 clones for at least 2 or more animals in both the vehicle

and mWTX-330 treated groups. X axis represents individual CDR3 sequences. C) Raw frequencies of individual TCR clones that were identified in the top 100 clones for at least 2 or more animals in exclusively the mWTX-330 treated groups. Data are presented as the mean  $\pm$  SD.

Supplemental Figure 10



### Supplemental Figure 10: mWTX-330 Treatment Increases the Mitochondrial Mass of Tumor Infiltrating Immune Cells and Does Not Impact Stemness Markers

EMT-6 tumor bearing mice were dosed twice a week with mWTX-330 or vehicle and tumors were collected on day 11 for analysis. Pathway analysis was performed on tumor infiltrating CD8+ T cells and heatmaps of genes associated with (A) glycolysis, (B) mitochondrial biogenesis, or (C) mitochondrial translation were generated (Supp Table 4). (D) Representative gating scheme for the identification of CD8+ T cells and NK cells. (E) CD4+ T cells from either vehicle or mWTX-330 treated animals were stained with Mitotracker Red. (F) TILs from either vehicle or mWTX-330 treated animals were stained with Mitotracker Green. EMT-6 infiltrating CD8+ T cells were assessed on day 11 for expression of (G) TCF7, (H) FOXO1, or (I) CD25.



Data are presented a box and whiskers plot, with the middle line representing the group mean, and p values are derived from t tests (\*,  $p < 0.05$ ; \*\*,  $p < 0.01$ ; \*\*\*\*,  $p < 0.0001$ ).